Dual Role of the Adaptive Immune System in Liver Injury and Hepatocellular Carcinoma Development

Highlights

- Flares of liver injury accelerate hepatocarcinogenesis

- The adaptive immune system has a dual role in chronic liver injury

- The immune system is not required for liver regeneration during chronic injury

- CD8^{+} T cells and LTβR contribute to hepatocarcinogenesis in chronic injury

Authors

Jessica Endig,
Laura Elisa Buitrago-Molina,
Silke Marhenke, ..., Thomas Longerich,
Mathias Heikenwälder, Arndt Vogel

Correspondence

vogel.arndt@mh-hannover.de

In Brief

Endig et al. show that T lymphocytes play dual roles in hepatic injury and tumor development, both being suppressed in alymphoid *Fah*^{−/−} mice despite increase in overall mortality. Depletion of CD8^{+} T cells or inhibiting the lymphotoxin-β receptor delays tumors development in mice with chronic liver damage.

Accession Numbers

GSE80459

CrossMark

CellPress

Article

Dual Role of the Adaptive Immune System in Liver Injury and Hepatocellular Carcinoma Development

Jessica Endig,[1,13] Laura Elisa Buitrago-Molina,[1,13] Silke Marhenke,[1,13] Florian Reisinger,[2] Anna Saborowski,[1] Jutta Schütt,[3] Florian Limbourg,[4] Christian Könecke,[5] Alina Schreder,[5] Alina Michael,[1] Ana Clara Misslitz,[1] Marc Eammonn Healy,[6] Robert Geffers,[7] Thomas Clavel,[8] Dirk Haller,[8] Kristian Unger,[9] Milton Finegold,[10] Achim Weber,[6] Michael P. Manns,[1] Thomas Longerich,[11] Mathias Heikenwälder,[3,12] and Arndt Vogel[1,*]

[1]Department of Gastroenterology, Hepatology and Endocrinology, Hannover Medical School, 30625 Hannover, Germany
[2]Institute of Virology, Technische Universität München, Helmholtz Zentrum Muenchen, 85764 Munich, Germany
[3]Department of Cardiology, Philipps University Marburg, 35037 Marburg, Germany
[4]Department of Nephrology and Hypertension
[5]Department of Hematology, Hemostasis, Oncology and Stem Cell Transplantation
Hannover Medical School, 30625 Hannover, Germany
[6]Institute of Surgical Pathology, University Hospital Zurich, 8091 Zürich, Switzerland
[7]Department of Cell Biology, Helmholtz Centre for Infection Research, 38124 Braunschweig, Germany
[8]ZIEL Institute for Food and Health, Technische Universität München, 85764 Munich, Germany
[9]Research Unit Radiation Cytogenetics, Helmholtz Zentrum München, 85764 Munich, Germany
[10]Department of Pathology, Texas Children's Hospital, Houston, TX 77030, USA
[11]Institute of Pathology, Aachen University Hospital, 52074 Aachen, Germany
[12]Division of Chronic Inflammation and Cancer, German Cancer Research Center Heidelberg, 69121 Heidelberg, Germany
[13]Co-first author
*Correspondence: vogel.arndt@mh-hannover.de
http://dx.doi.org/10.1016/j.ccell.2016.06.009

SUMMARY

Hepatocellular carcinoma (HCC) represents a classic example of inflammation-linked cancer. To characterize the role of the immune system in hepatic injury and tumor development, we comparatively studied the extent of liver disease and hepatocarcinogenesis in immunocompromised versus immunocompetent Fah-deficient mice. Strikingly, chronic liver injury and tumor development were markedly suppressed in alymphoid $Fah^{-/-}$ mice despite an overall increased mortality. Mechanistically, we show that CD8$^+$ T cells and lymphotoxin β are central mediators of HCC formation. Antibody-mediated depletion of CD8$^+$ T cells as well as pharmacological inhibition of the lymphotoxin-β receptor markedly delays tumor development in mice with chronic liver injury. Thus, our study unveils distinct functions of the immune system, which are required for liver regeneration, survival, and hepatocarcinogenesis.

INTRODUCTION

Hepatocellular carcinoma (HCC) is one of the most lethal and prevalent cancers worldwide and has recently become the second most common cause for cancer-related death in humans. In contrast to many other cancers, its incidence increases annually by 1.75% in the Western world. HCC is commonly caused by hepatitis B and C infections (~75%), and is less frequently associated with chronic exposure to toxins or hereditary liver diseases (El-Serag et al., 2008). Although many studies have reported significant alterations in inflammatory cells and in the expression of different cytokines in liver cirrhosis and HCC, the critical components linking inflammation and hepatocarcinogenesis are only beginning to be unraveled.

The liver is heavily populated by immune cells, including macrophages, natural killer (NK) cells, NKT cells, and CD4$^+$ and CD8$^+$

Significance

Tumors frequently arise in the context of inflammation, which is increasingly recognized as a key factor in the pathogenesis of malignancies. Although activation of different cytokines has been reported in liver diseases, the critical components linking inflammation and hepatocarcinogenesis remain elusive. We demonstrate that lymphocytes play a decisive, yet ambiguous role in chronic liver disease; while infiltrating lymphocytes mediate hepatocyte damage, liver fibrosis, and tumor development, they also protect mice from acute-on-chronic liver failure. Our data illustrate that the immune system needs to be tightly regulated in a context-specific fashion to balance immune surveillance and cancer risk. We propose that targeting tumor-promoting pathways such as LTβ might be an attractive chemopreventive strategy for patients at risk.

T cells. The co-residence of these immune cells in the liver creates a unique environment that regulates liver homeostasis. Experimental studies with rodents suggest that T and NK cells are not only required to eliminate pathogenic microorganisms but that they also regulate liver regeneration by supporting proliferation of hepatocytes and hepatic progenitor cells under non-infectious conditions (Strick-Marchand et al., 2004; Tumanov et al., 2009). Moreover, sustained inflammation may not only create an environment in which the continuous presence of pro-proliferative stimuli ultimately leads to liver fibrosis and cirrhosis, but may also contribute to the malignant transformation of hepatocytes. In this regard, there is evidence that lymphocyte-derived cytokines such as lymphotoxin β (LTβ) and tumor necrosis factor-α (TNF-α) are involved in viral hepatitis and cholestasis-induced hepatocarcinogenesis, as well as in the progression of non-alcoholic steatohepatitis to HCC (Haybaeck et al., 2009; Pikarsky et al., 2004; Wolf et al., 2014).

On the contrary, the immune system is able to launch a potent anti-tumor response in the process of liver carcinogenesis, exemplified by the observation that progression of hepatic tumors is strikingly enhanced in T and B cell-deficient $Rag1^{-/-}$ mice upon treatment with the chemical carcinogen DEN (Schneider et al., 2012). Similarly, impaired immune surveillance of pre-malignant senescent hepatocytes has been shown to lead to the development of murine HCCs, suggesting that senescence surveillance is important for tumor suppression in the liver (Kang et al., 2011; Ma et al., 2016).

To further delineate the role of the immune system in the liver during chronic injury and to specify its role in the initiation and progression of HCC, we used a mouse model of hereditary tyrosinemia type 1 (HT1). HT1 is an autosomal recessive human disease caused by a genetic inactivation of the enzyme fumarylacetoacetate hydrolase (FAH), which catalyzes the last step in the tyrosine degradation and is predominantly expressed in liver and kidneys. This defect leads to an accumulation of toxic metabolites such as fumarylacetoacetate (FAA), which subsequently causes acute and chronic liver failure (Grompe et al., 1993). The drug NTBC (2-[2-nitro-4-(trifluoromethyl)benzoyl] cyclohexane-1,3-dione, or Nitisinone), which blocks the pathway upstream of FAA formation, is used to treat patients with HT1 and prevents liver injury in $Fah^{-/-}$ mice (Grompe et al., 1995; Mayorandan et al., 2014). The murine model of Fah-deficiency reliably mirrors the inflammatory environment of the human disease and is therefore suitable to delineate the divergent roles of immune cells in chronic liver injury, and has been extensively used to study liver carcinogenesis and regeneration (Buitrago-Molina et al., 2009; Marhenke et al., 2008; Willenbring et al., 2004, 2008).

RESULTS

Activation of the Intrahepatic Immune Cells in FAA-Induced Liver Injury

HCC represents a classic case of inflammation-linked cancer, and chemically or genetically induced HCC is highly dependent on inflammatory signaling. Repeated flares of injury typically characterize chronic human liver diseases. Using the FAH model as a surrogate for chronic liver disease, we first aimed to phenotype the infiltrating immune cells upon repeated FAA-induced liver injury. As described in detail in Figure S1, NTBC was withdrawn for 3 weeks and subsequently re-administered for 5 days to allow recovery and liver regeneration. Flares of liver injury were repeated up to six times. FAA-induced liver injury was accompanied by a strong increase in $CD3^+$ $CD4^+$ and $CD3^+$ $CD8^+$ T cells compared with mice on 100% NTBC, whereas $B220^+$ $CD19^+$ B cells remained unchanged (Figures 1A and 1D). The majority of $CD4^+$ and $CD8^+$ T cells were effector memory T cells ($CD44^{hi}$ $CD62L^{lo}$) and also expressed CD69 as a marker of T cell activation (Figures 1B and 1C). In addition, we observed a non-significant increase in ($CD3^-$ $NK1.1^+$) NK and ($CD3^+$ $NK1.1^+$) NKT cells (Figures 1E and 1F).

Following acute liver injury, infiltrating bone marrow-derived monocytes massively expand the pool of macrophages. Resident Kupffer cells and infiltrating macrophages are CD11b- and F4/80-expressing cells in mice. Here, liver injury was accompanied by a strong increase of myeloid cells as shown by F4/80 fluorescence-activated cell sorting (FACS) analysis and CD11b and F4/80 immunostaining (Figures 1G and 1H). FACS analysis of the spleen and blood revealed a similar activation of immune cells suggesting a systemic immune response (data not shown).

The Adaptive Immune System Is Required for the Survival of Fah-Deficient Mice with Liver Injury

We chose to take a comprehensive approach to address the impact of the immune system on chronic liver injury. $Fah^{-/-}$ $Rag2^{-/-}$ $Il2r\gamma^{-/-}$ (FCR) mice, which lack all lymphoid cells including NK and NKT cells, were generated. Healthy FCR mice on 100% NTBC treatment did not display any overt morphological or biochemical phenotype. Flares of liver injury were induced by repeated NTBC withdrawal in $Fah^{-/-}$ and FCR mice. In the $Fah^{-/-}$ cohort, 55% of experimental animals survived the repeated NTBC withdrawal (median overall survival ≈121 days, n = 31) (Figure 2A). Survival of FCR mice was dramatically reduced compared with $Fah^{-/-}$ mice (median overall survival ≈31 days, n = 35, hazard ratio [HR] 0.31, p ≤ 0.05). Approximately 70% of the FCR mice died within the first 2 months, thus implicating that the immune system serves an important pro-survival function during chronic liver injury.

To further delineate the role of the immune system in FAA-induced liver injury, we comparatively analyzed livers of $Fah^{-/-}$ and FCR mice following the second course of NTBC withdrawal. As expected, H&E staining revealed moderate to severe acinar inflammation, numerous ballooned, and some dysplastic hepatocytes with nuclear polymorphism and multi-nucleation in $Fah^{-/-}$ mice without NTBC (0%) treatment (Figure 2B). Necrosis was the main mechanism of hepatocyte death and there was hardly any evidence of apoptosis, with only a few scattered TUNEL- and cleaved caspase 3-positive hepatocytes (Figure 2C). Elevated bilirubin and aspartate transaminase (AST) levels accompanied histological liver injury (Figures 2D and 2E). In contrast, liver damage was significantly reduced in the surviving FCR mice. To histologically quantify and compare chronic liver injury we assessed the modified Ishak Score, further confirming a markedly increased histological remodeling in the livers of $Fah^{-/-}$ mice compared with immunosuppressed FCR mice (Figure 2E). Accordingly, bilirubin and transaminase levels
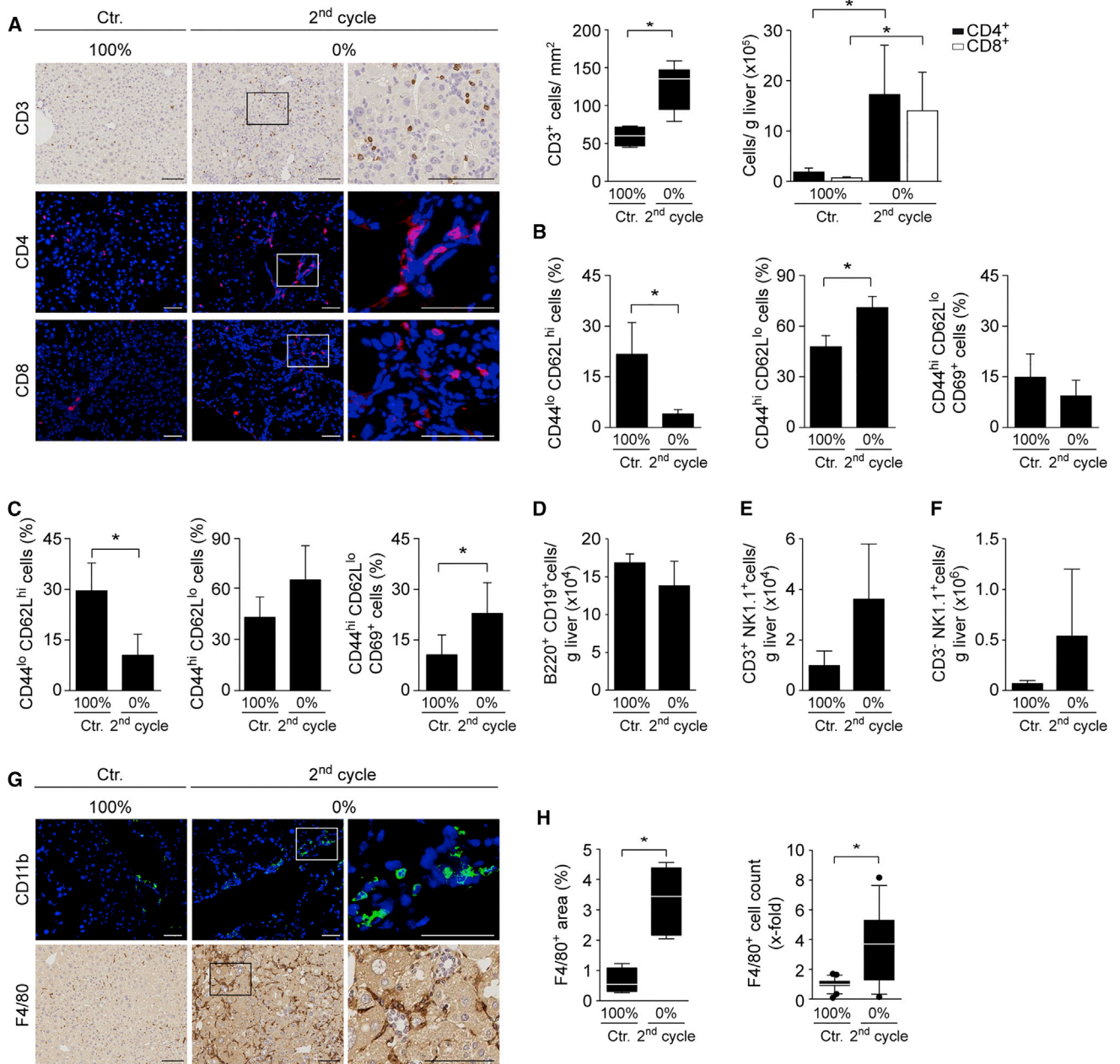
Figure 1. Activation of the Immune System in *Fah*⁻/⁻ Mice

(A–F) *Fah*⁻/⁻ mice were either exposed to two courses of NTBC withdrawal (0% NTBC) and re-supplementation or continuously kept on 100% NTBC.
(A) Representative IHC and corresponding quantification of liver-infiltrating $CD3^+$, $CD4^+$, and $CD8^+$ cells. Flow cytometric analysis of T cells ($CD4^+$ and $CD8^+$),
(D) B cells ($B220^+$ $CD19^+$), (E) NK cells ($CD3^-$ $NK1.1^+$), and (F) NKT cells ($CD3^+$ $NK1.1^+$) following NTBC withdrawal. Immunophenotyping of (B) $CD4^+$ and (C) $CD8^+$ T cells for the homing marker CD62L and CD44 and the activation marker CD69 by FACS.
(G) Representative IHC on liver sections for the myeloid cell markers CD11b and F4/80.
(H) Boxplots depict the increase in $F4/80^+$ cells quantified in area or assessed by FACS analysis (relative to controls). Magnified views from IHC are shown in boxes.
Data represent mean ± SD (or ±SEM for B cells' plot) or median with whiskers from 10th to 90th percentiles. *$p \leq 0.05$. Scale bars represent 100 μm. See also Figure S1.

were only marginally increased in the serum of FCR mice (Figures 2D and 2E). We have previously shown that FAA-induced liver damage leads to a strong, protective activation of the Nrf2 pathway, reflected by the increased expression of

NAD(P)H dehydrogenase 1 (NQO1) and heme oxygenase-1 (HO-1) (Marhenke et al., 2008). Both proteins were significantly upregulated in livers of cycled *Fah*⁻/⁻ and FCR mice (Figure S2), indicating that hepatocytes in *Fah*⁻/⁻ and FCR mice experience
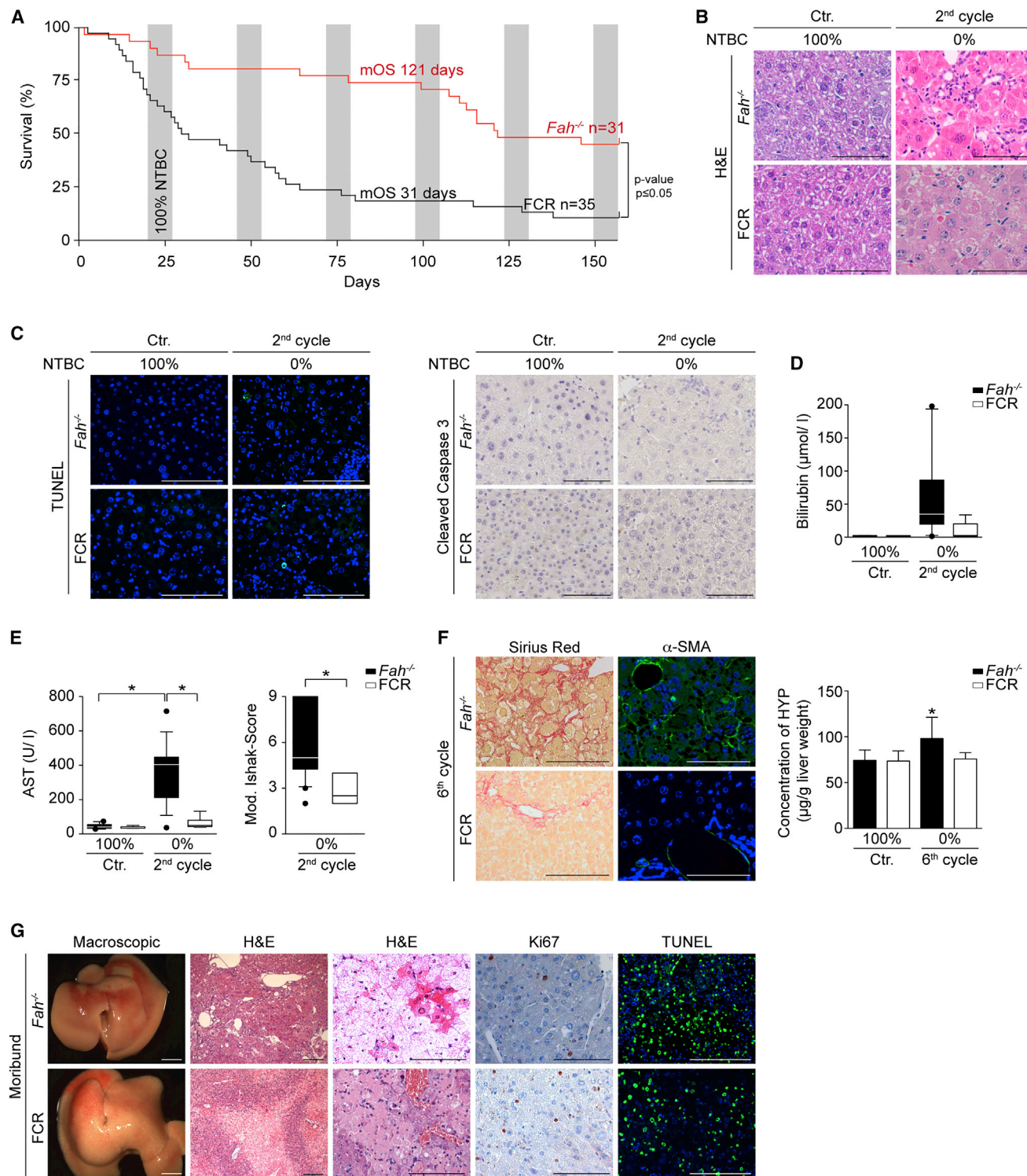
Figure 2. The Adaptive Immune System Is Required for the Survival of Fah-Deficient Mice with Liver Injury

(A) $Fah^{-/-}$ and FCR mice were cycled six times. Kaplan-Meier plot shows the reduced survival of FCR mice compared with immunocompetent $Fah^{-/-}$ mice (median overall survival [mOS] = 121 and 31 days, respectively).

(B–E) $Fah^{-/-}$ and FCR mice were cycled two times (0%) or kept on 100% NTBC. Representative images from H&E (B), TUNEL and cleaved caspase-3 (C) staining on liver sections were taken. (D and E) Markers of cholestasis (bilirubin) and hepatocyte injury (AST) are almost exclusively elevated in the serum of $Fah^{-/-}$ mice undergoing repeated NTBC withdrawal. (E) The modified Ishak Score was assessed to histologically quantify inflammation and fibrosis.

a similar degree of oxidative stress inflicted by the accumulation of FAA.

Long-term FAA-induced liver injury caused progressive biliary fibrosis in $Fah^{-/-}$ mice. Extensive interstitial collagen deposition, determined by Sirius red staining, and an increase of α-smooth muscle actin (α-SMA)-positive stellate cells was evident in $Fah^{-/-}$ mice after six courses of NTBC withdrawal (Figure 2F). The degree of fibrosis was quantified by measuring the hepatic content of hydroxyproline, which was significantly elevated in livers of cycled $Fah^{-/-}$ mice compared with healthy mice on 100% NTBC (Figure 2F, p ≤ 0.05). In agreement with the significantly reduced liver damage, there was no evidence of liver fibrosis in FCR mice (Figure 2F).

To understand the increased mortality in FCR mice despite less pronounced liver injury in mice with long-term survival, we harvested several mice when showing signs of rapidly deteriorating health and weight loss of more than 20%. Macroscopically, livers of moribund mice appeared pale. Contrary to our observations in healthy FCR mice undergoing NTBC withdrawal, H&E and TUNEL staining revealed massive hepatic necrosis and apoptosis without any signs of liver regeneration, suggesting that these mice died from acute-on-chronic liver failure (Figure 2G). Areas of liver necrosis were surrounded and infiltrated by neutrophils. Livers from moribund mice of both cohorts showed a comparable histology, independent of whether the mice required euthanasia after days or weeks of repetitive cycling. No bacteria or fungi were detected in livers of harvested mice by Gram or silver staining (data not shown). Moreover, there were no signs of hepatic vascular or perfusion disorder in mice of both genotypes.

Together, these data indicate that the immune system has a context-dependent role, which is exemplified by the observations that $Fah^{-/-}$ mice that survive over 4 months display more pronounced liver injury and fibrosis in comparison with immunosuppressed FCR mice. On the contrary, the adaptive immune system prevents early death in immnocompetent $Fah^{-/-}$ mice, while 70% of FCR mice die within 2 months.

The Adaptive Immune System Is Not Required for Liver Regeneration in Fah-Deficient Mice with Liver Injury

We have previously shown that complete NTBC withdrawal results in a strong induction of p21 protein expression, leading to an almost complete cell-cycle arrest in Fah-deficient hepatocytes (Buitrago-Molina et al., 2013; Willenbring et al., 2008). Accordingly, a pronounced activation of the p21 pathway and almost no Ki67-positive hepatocytes were observed in $Fah^{-/-}$ mice after NTBC withdrawal (second cycle) despite a clear induction of cyclin D1 (Figures 3A and 3B). In the recovery phase, a dramatic increase of proliferating hepatocytes was evident (Figure 3A) (Ki67 labeling index of 36.6% in mice re-supplemented with NTBC compared with 0% in mice taken off NTBC, p ≤ 0.05). These findings were further confirmed by

increased bromodeoxyuridine incorporation and histone H3 phosphorylation (data not shown). Comparable results were obtained in FCR mice upon NTBC withdrawal and reconstitution. However, in agreement with the reduced liver injury in FCR mice, the proliferation rate of hepatocytes in response to NTBC re-supplementation was significantly lower than in $Fah^{-/-}$ mice (Figure 3A, p ≤ 0.05).

It is generally accepted that increased proliferation of hepatocytes is a key contributor to liver regeneration. In addition, hypertrophy of hepatocytes was recently identified as an additional mechanism of liver regeneration following partial hepatectomy. The circumference of hepatocytes can be visualized by β-Catenin staining, and hepatocytes can be distinguished from other non-parenchymal cells based on their size (Figure 3C). Quantitative analysis revealed that the size of hepatocytes more than doubled in $Fah^{-/-}$ mice taken off NTBC. Accordingly, the number of hepatocytes significantly dropped by more than 50% per field of vision in $Fah^{-/-}$ mice (Figure 3C). Liver weight of $Fah^{-/-}$ mice decreased by 24%, indicating loss of more than 60% of hepatocytes upon NTBC withdrawal (data not shown). During NTBC re-treatment, the size of hepatocytes slightly decreased and hepatocyte counts slightly increased compared with mice off NTBC. Intriguingly, cell size and number were maintained in FCR mice during NTBC cycling, in agreement with the reduced liver injury (Figure 3C).

Considering that liver progenitor cells (LPCs) located within the smallest branches of the intrahepatic biliary tree are activated upon liver injury, we decided to assess the presence of progenitor cells in $Fah^{-/-}$ and FCR mice using the established LPC markers A6 and MIC1-1C3 (Dorrell et al., 2011). Importantly, these markers are also expressed by regular cholangiocytes, serving as an internal staining control (Tarlow et al., 2014). Indeed, a marked increase of A6-positive LPCs was present in the livers of $Fah^{-/-}$ mice (Figure 3D). Moreover, FACS analysis confirmed a significant increase of CD45⁻/CD11b⁻/CD31⁻/TER119⁻/MIC1-1C3⁺/CD133⁻ and CD45⁻/CD11b⁻/CD31⁻/TER119⁻/MIC1-1C3⁺/CD133⁺ LPCs in these livers (Figure 3E). Notably, the LPC response was completely abrogated in cycled FCR mice, suggesting that the immune system is required for activation of LPCs (Figures 3D and 3E).
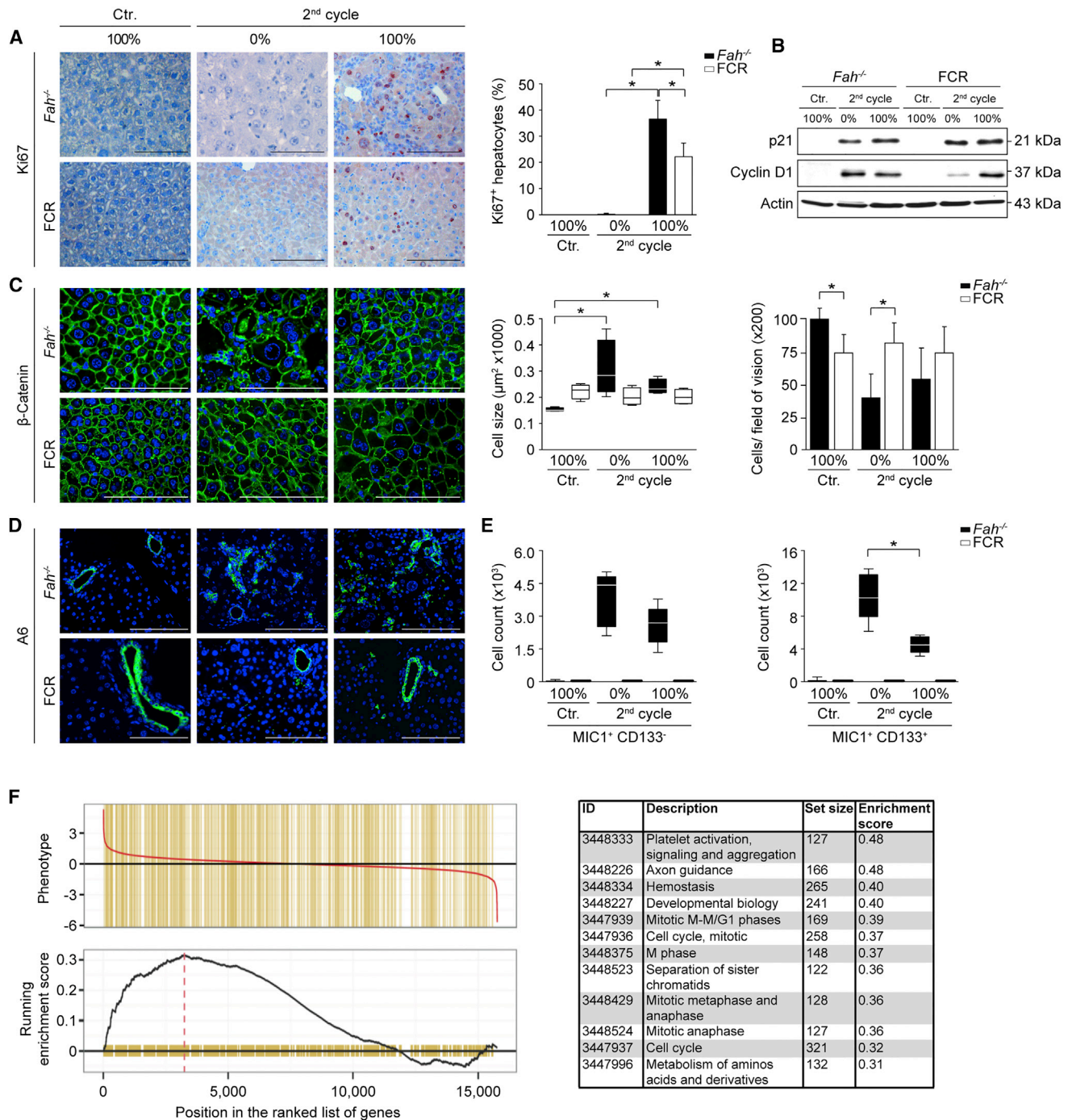
To better understand how the immune system modulates the cellular stress response and to identify gene-expression profiles, we performed microarray analysis and gene set enrichment analysis on livers from cycled $Fah^{-/-}$ and FCR mice and their respective controls. The most significantly differently regulated categories in cycled $Fah^{-/-}$ compared with cycled FCR mice and healthy $Fah^{-/-}$ mice on 100% NTBC were related to "cell cycle," in agreement with the strong proliferative response in the recovery phase of $Fah^{-/-}$ mice (Figure 3F).

Together, these data indicate that liver regeneration during chronic injury is accomplished by proliferation of hepatocytes, hepatocyte hypertrophy, and activation of LPCs. Liver

---

(F) Livers from $Fah^{-/-}$ and FCR mice were harvested after six cycles. Sirius red and α-SMA staining revealed advanced fibrosis in livers of immunocompetent $Fah^{-/-}$ mice, correlating with an increase in hepatic hydroxyproline content.

(G) $Fah^{-/-}$ and FCR mice were harvested upon signs of deteriorating health. Macroscopically livers were pale with large areas of necrosis (H&E) and apoptosis (TUNEL) without proliferating hepatocytes (Ki67).

Data represent means ± SD or median with whiskers from 10th to 90th percentiles. *p ≤ 0.05. Scale bars represent 100 μm, except for macroscopic pictures (5 mm). See also Figure S2.

A

Ctr. | 2nd cycle
100% | 0% | 100%

Ki67

Fah−/−

FCR

Ki67+ hepatocytes (%)

■ Fah−/− □ FCR

B

Fah−/− | FCR
Ctr. | 2nd cycle | Ctr. | 2nd cycle
100% | 0% | 100% | 100% | 0% | 100%

p21 — 21 kDa
Cyclin D1 — 37 kDa
Actin — 43 kDa

C

β-Catenin

Fah−/−

FCR

Cell size (µm² x1000)

100% | 0% | 100%
Ctr. | 2nd cycle

Cells/ field of vision (x200)

■ Fah−/− □ FCR

100% | 0% | 100%
Ctr. | 2nd cycle

D

A6

Fah−/−

FCR

E

■ Fah−/− □ FCR

Cell count (x10³)

100% | 0% | 100%
Ctr. | 2nd cycle
MIC1+ CD133−

Cell count (x10³)

100% | 0% | 100%
Ctr. | 2nd cycle
MIC1+ CD133+

F

Phenotype

Running enrichment score

0 | 5,000 | 10,000 | 15,000
Position in the ranked list of genes

| ID	Description	Set size	Enrichment score
3448333	Platelet activation, signaling and aggregation	127	0.48
3448226	Axon guidance	166	0.48
3448334	Hemostasis	265	0.40
3448227	Developmental biology	241	0.40
3447939	Mitotic M-M/G1 phases	169	0.39
3447936	Cell cycle, mitotic	258	0.37
3448375	M phase	148	0.37
3448523	Separation of sister chromatids	122	0.36
3448429	Mitotic metaphase and anaphase	128	0.36
3448524	Mitotic anaphase	127	0.36
3447937	Cell cycle	321	0.32
3447996	Metabolism of aminos acids and derivatives	132	0.31

Figure 3. The Adaptive Immune System Is Not Required for Liver Regeneration in Fah-Deficient Mice with Liver Injury

(A–F) $Fah^{-/-}$ and FCR mice were cycled twice and livers were collected after the off (0% NTBC) and on phases (100% NTBC), respectively. (A) Ki67 IHC was performed and stained nuclei were quantified. (B) Immunoblot showing increased expression of p21 and cyclin D1 in both $Fah^{-/-}$ and FCR mice upon liver injury (pooled liver homogenates, n = 6). (C) β-Catenin staining was performed to determine hepatocyte size and calculate the number of cells per field of vision. In contrast to FCR mice, multiple LPCs are detectable in immunocompetent $Fah^{-/-}$ mice by A6 IHC (D) and FACS (MIC1-1C3+ and MIC1-1C3+ CD133+ cells) (E). (F) Gene set enrichment analyses revealed an upregulation of cell-cycle signature genes in hepatic $Fah^{-/-}$ cells. Significantly enriched signatures in $Fah^{-/-}$ liver cells are summarized in the table.

Data represent mean ± SD or median with whiskers from minimum to maximum values. *p ≤ 0.05. Scale bars represent 100 µm.
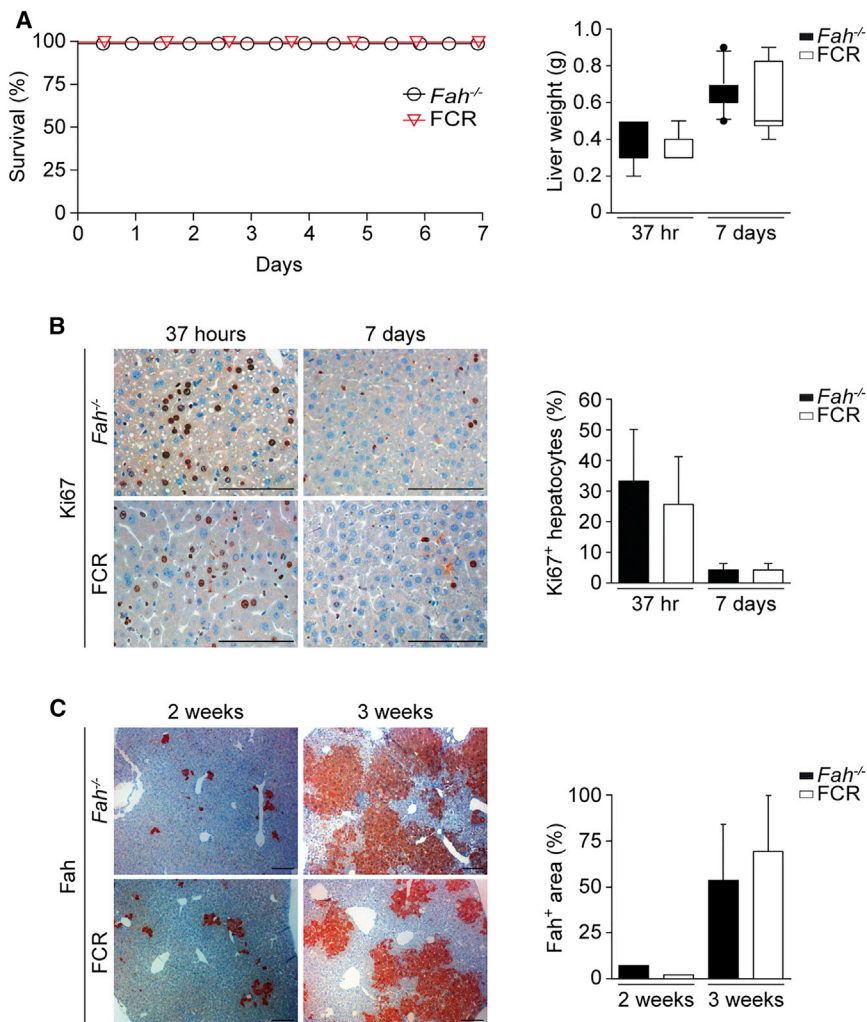
Figure 4. The Adaptive Immune System Is Not Required for Cell-Cycle Progression in Fah-Deficient Hepatocytes in Response to Partial Hepatectomy or after Hepatocyte Transplantation

(A and B) Loss of the adaptive immune system does not compromise survival following PH. Two-thirds partial hepatectomy was performed in healthy $Fah^{-/-}$ and FCR mice on NTBC. (A) Kaplan-Meier plot showing the survival rates after PH. Liver weight was measured 37 hr and 7 days after PH. (B) Ki67 staining at 37 hr and 7 days after PH and quantification of Ki67-positive, proliferating hepatocytes.

(C) Hepatocytes isolated from 6-week-old C57BL/6N mice were transplanted into $Fah^{-/-}$ and FCR mice by intrasplenic injection. Re-population efficiency of wild-type hepatocytes was determined by Fah IHC and the area of Fah-positive hepatocytes was assessed.

Data represent mean ± SD or median with whiskers from 10th to 90th percentiles. Scale bars represent 100 μm.

compromised $Fah^{-/-}$ mice (Figure 4A). As expected, multiple Ki67+ cells were clearly visible 37 hours after PH in 3-month-old $Fah^{-/-}$ mice as well as in FCR mice. There was no significant difference in the Ki67 labeling index between the immunocompetent and immunocompromised cohort (Figure 4B).

Next, WT hepatocytes were transplanted into $Fah^{-/-}$ and FCR mice. Subsequently, NTBC supplementation was withdrawn, thereby creating a strong proliferative environment for transplanted Fah-expressing cells. This experimental approach allowed us to specifically analyze how the microenvironment affects cell-cycle progression in normal WT hepatocytes. Following transplantation, multiple proliferating hepatocytes were detectable in liver sections of all groups. Fah immunostaining revealed that WT hepatocytes re-populated livers of $Fah^{-/-}$ and FCR mice with comparable efficiency (Figure 4C). Thus, the transplantation experiments confirmed that the adaptive immune system is not required for effective engraftment and proliferation of hepatocytes in livers with chronic injury.

regeneration by self-duplication of hepatocytes is not impaired in immunosuppressed $Fah^{-/-}$ mice, whereas the immune system is required for full activation of the LPC response.

The Adaptive Immune System Is Not Required for Cell-Cycle Progression in Fah-Deficient Hepatocytes in Response to Partial Hepatectomy or Following Hepatocyte Transplantation

Based on experiments in $Rag2^{-/-}$ mice, which are devoid of B, T, and NKT cells, Tumanov and colleagues postulate that the adaptive immune system is required for liver regeneration in wild-type (WT) mice following partial hepatectomy (Tumanov et al., 2009). To further analyze the role of the adaptive immune system in healthy Fah-deficient hepatocytes, we performed two-thirds partial hepatectomy and hepatocyte transplantation experiments on $Fah^{-/-}$ and FCR mice maintained on 100% NTBC supplementation. All mice in both groups survived the partial hepatectomies, indicating that loss of the adaptive immune system does not compromise survival following PH (Figure 4A). Moreover, recovery of liver mass 1 week following PH was similar in both groups, confirming that there is no significant impact on liver regeneration following PH in immuno-

Tumor Development Is Markedly Suppressed in Immunodeficient $Fah^{-/-}$ Mice with Chronic Liver Injury

To study the role of the immune system in chronic FAA-induced liver injury, we analyzed livers following the second, fourth, and sixth cycle of NTBC withdrawal. Several studies suggest that most malignant tumors are most likely derived from single progenitor cells that have acquired genetic and epigenetic changes that allow clonal expansion. Recently, CD44+ HCC progenitor cells have been identified in different HCC mouse models (He et al., 2013). In contrast to HCC-derived cancer cells, these progenitor cells solely give rise to tumors in mice with chronic liver
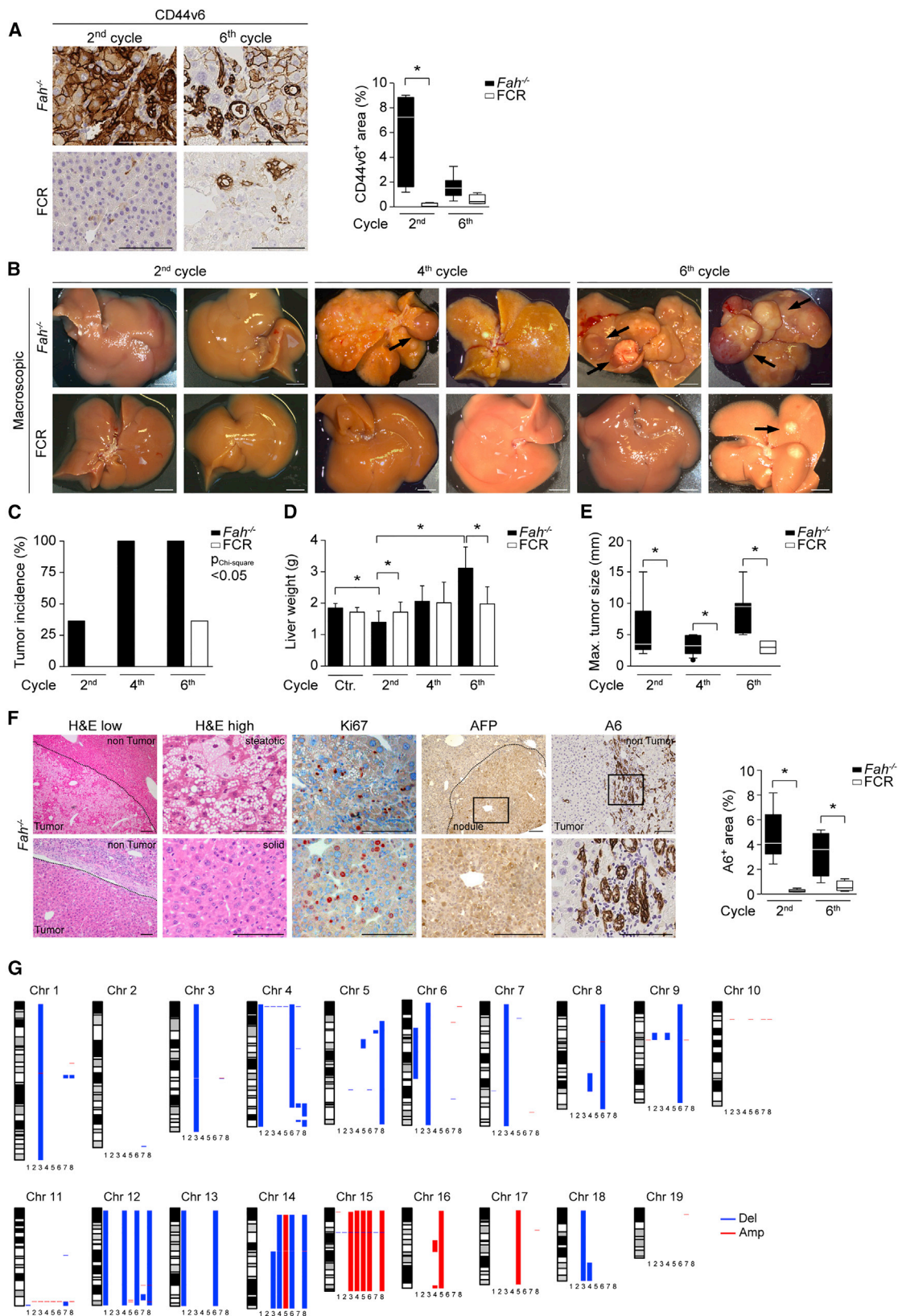
(legend on next page)

injury. In our model, liver sections from $Fah^{-/-}$ mice showed the progressive appearance of CD44v6$^+$ cells whereas these cells did not increase in immunosuppressed mice, suggesting that FAA-induced liver injury only gives rise to bona fide HCC-initiating cells in immune-competent mice (Figure 5A).

Ongoing proliferation of hepatocytes and progenitor cells during the recovery phase allowed rapid progression to frank HCCs. 33% of $Fah^{-/-}$ mice had already developed small tumor nodules after the second cycle (n = 22). After the fourth and sixth cycles, HCCs were present in all mice (n = 28) (Figures 5B and 5C), and tumor growth was accompanied by a significant increase in liver weight after the sixth cycle (Figures 5D and 5E). By this time, the mean size of the largest tumor nodule per liver had increased from 5.6 mm after the second cycle to 8.8 mm (Figure 5E). Histological examination of the livers confirmed the presence of numerous dysplastic hepatocytes and moderately to well-differentiated HCCs with fatty changes and solid growth pattern (Figure 5F). Multiple Ki67$^+$ and AFP$^+$ tumor cells were observed within the tumor lesions. A6$^+$ and CD44v6$^+$ cells surrounded the tumors at the border zone, but were not present within the tumors (Figures 5A and 5F).

In contrast, HCC development was significantly reduced in FCR mice, with only 12% harboring detectable tumors within the first sixth cycles (Figures 5B and 5C). Accordingly, liver weight and mean size of tumors were significantly lower in these mice compared with the $Fah^{-/-}$ mice (Figures 5D and 5E). Microdissected HCCs (n = 8) and age-matched control livers (n = 4) were investigated for chromosomal aberrations by array comparative genomic hybridization analysis (aCGH). The most common loss that was present in all eight profiles was a small region on chromosome 15 (gene Ctnnd2), and in seven of eight profiles an unknown gene on chromosome 4. In four of eight cases the analysis of chromosomal aberrations showed losses of whole chromosome (chromosomes 12 and 14). Most frequent gains were a small region on chromosome 11 (six of eight, gene St6galnac1), whole chromosome 15 (five of eight), and small regions on chromosome 10 (four of eight, genes Raetie and H60b) and chromosome 15 (four of eight, genes Sepp1, Ghr, Fbxo4, Oxtc1, Plcxd3, and C6) (Figure 5G). A representation of identified genomic copy-number alterations can be found in Table S1. Synteny analyses revealed that approximately 80% of the genomic alterations found in $Fah^{-/-}$ tumors were congruent with loci changed in human HCCs. A high degree of overlap was observed between copy-number alterations that were determined in our mouse model and human alcohol-induced HCCs or HCCs with c-myc alterations (overlap gains/losses alcohol-induced HCCs, 70.6%/79.1%; HCCs with c-myc alteration, 75.7%/79.5%; p $\leq$ 0.0001 for all comparisons) (Table S2 and Figure S3).

Taken together, NTBC cycling with repeated phases of compensatory proliferation facilitates rapid progression to HCCs in $Fah^{-/-}$ mice. In contrast, hepatocarcinogenesis is markedly suppressed in alymphoid mice, indicating that adaptive immune cells critically promote hepatocarcinogenesis.

Adoptive Transfer of T Cells Reduces Acute-on-Chronic Liver Failure in Immunosuppressed $Fah^{-/-}$ Mice

FCR mice are devoid of all lymphoid cells. To further delineate, which cells contribute to FAA-induced liver injury, regeneration, and hepatocarcinogenesis, we generated $Fah^{-/-}$ $Rag2^{-/-}$ (FR) mice, lacking mature B and T lymphocytes, and $Fah^{-/-}$ $\beta 2m^{-/-}$ (Fβ2m) mice, lacking CD8$^+$ T and NKT cells. FR mice were analyzed after four to five rounds of cycling to elucidate the role of the NK1.1$^+$ cells. To specifically analyze the role of NKT and CD8$^+$ T cells, we compared Fβ2m mice with $Fah^{-/-}$ mice. Similarly to the FCR mice, the mortality of the FR and Fβ2m mice was significantly increased (median overall survival of FR $\approx$ 18.5 days, n = 16, HR 0.28, p $\leq$ 0.05; median overall survival of Fβ2m $\approx$ 20 days, n = 18, HR 0.30, p $\leq$ 0.05, respectively), suggesting that CD8$^+$ T cells protect $Fah^{-/-}$ mice from acute-on-chronic liver failure (Figure 6A). We next determined whether adoptive transfer of T cells into FCR and FR mice could rescue the hepatic phenotype. Flow cytometric analysis revealed a significantly lower number of T cells in adoptively transferred FCR mice compared with $Fah^{-/-}$ mice (data not shown), but these cells were sufficient to protect the immunosuppressed mice from the acute liver failure (Figure 6A). Next, mice were analyzed with respect to tumor development. No tumor development was detectable in FR, Fβ2m, and T cell transplanted FCR and FR mice. There were hardly any proliferating or apoptotic hepatocytes in cycled mice during the off phase, similar to $Fah^{-/-}$ and FCR mice (Figure 6B). Finally, the LPC response was abrogated in all mice that lacked T cells as indicated by the absence of A6-expressing cells (Figure 6B). In contrast, T cell transplantation was sufficient to stimulate an LPC response in FCR and FR mice. Moreover, LPCs were readily detectable in Fβ2m mice suggesting that CD4$^+$ T cells, which have previously been shown to co-localize with expanding and migrating oval cells (Strick-Marchand et al., 2008), are sufficient to activate LPCs during chronic liver injury.

Together, these data highlight the dual role of T cells in liver injury and HCC development. T cells are required to protect mice from the increased mortality observed in alymphoid mice. On the contrary, activation of T cells significantly contributes to liver injury and promotes tumor development. CD4$^+$ T cells are specifically required to allow LPC expansion in mice with chronic liver injury, whereas absence of adaptive immune cells does not preclude normal hepatocyte proliferation.

Figure 5. Tumor Development Is Markedly Reduced in Immunosuppressed Fah-Deficient Mice with Chronic Liver Injury

(A–G) $Fah^{-/-}$ and FCR mice were cycled twice, four, and six times. (A) Immunostaining revealed an increase of CD44v6-positive cells in $Fah^{-/-}$ mice. (B) Representative macroscopic pictures demonstrate multiple tumors in $Fah^{-/-}$ livers. Scale bars represent 5 mm. Examples of tumors are indicated with black arrows. Quantification of tumor incidence (C), liver weight (D), and maximal tumor size (E) are shown. (F) H&E staining of liver sections from tumor-bearing $Fah^{-/-}$ mice show well-differentiated HCCs with two distinct growth patterns. Dotted outlines mark tumor and non-tumor tissue. Multiple proliferating tumor cells are found in tumors (Ki67). Multiple AFP$^+$ and A6$^+$ progenitor cells are detectable in $Fah^{-/-}$ livers. Dotted outline marks a tumor nodule. Magnified views of boxed areas for AFP and A6 are shown. A6-positive area was quantified. Scale bars represent 100 μm. (G) An array comparative genomic hybridization analysis (aCGH) reveals numerous chromosomal aberrations in HCCs from $Fah^{-/-}$ mice.

Data represent mean ± SD or median with whiskers from minimum to maximum values. *p $\leq$ 0.05. See also Figure S3; Tables S1 and S2.
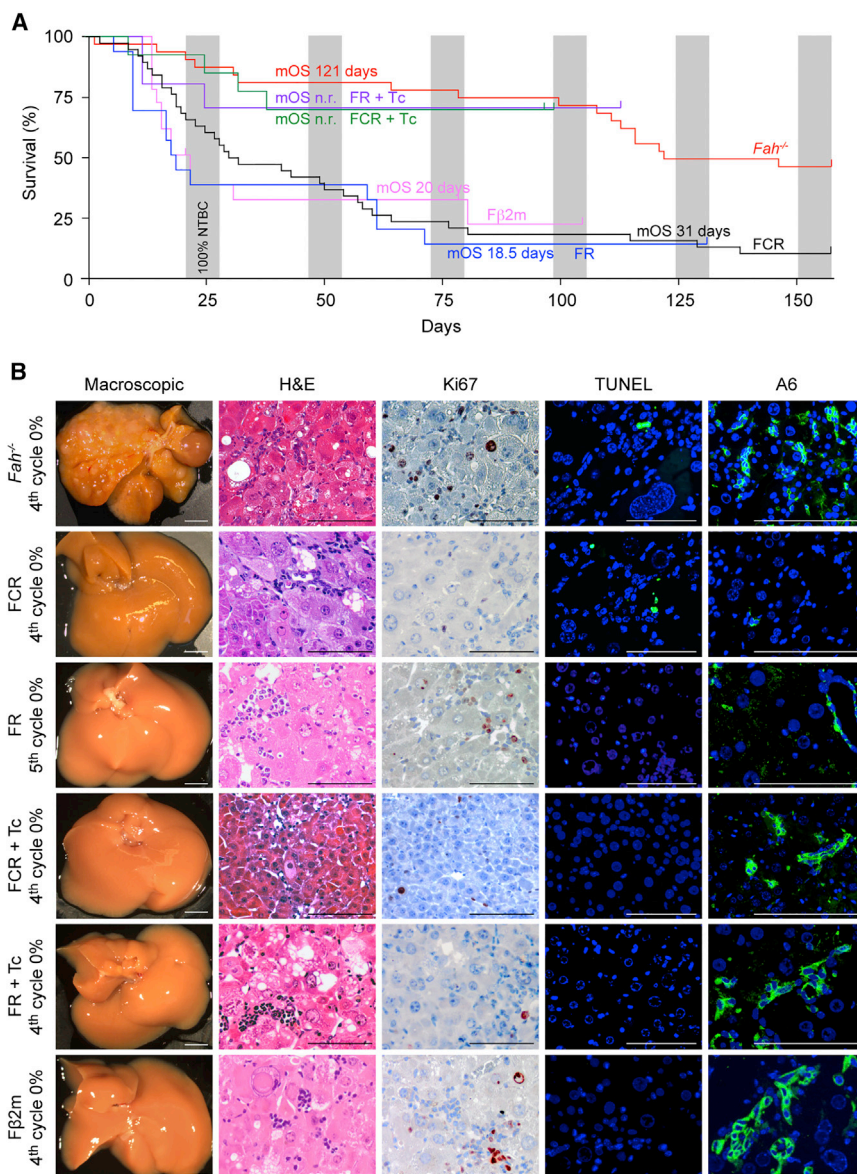
Figure 6. CD8+ T Cells Are Required for FAA-Induced Liver Disease and Hepatocarcinogenesis

(A and B) $Fah^{-/-}$ and FCR mice, as well as $F\beta 2m$ and FR were cycled. Mice with adoptive T cell transfer are denoted as "+Tc." (A) Kaplan-Meier plot showing the survival rates and median overall survival of all mice after repeated NTBC withdrawal. n.r., not reached. (B) Livers were harvested after four to five cycles in 0% NTBC phase and were immunohistochemically analyzed. Representative macroscopic pictures and H&E, Ki67, TUNEL, and A6 IHCs on liver sections are shown. Scale bars represent 100 μm, except for macroscopic pictures (5 mm).

most likely attributable to an impaired re-uptake of conjugated bilirubin into the liver caused by a reduced expression of the membrane transport proteins OATP1B1 and OATP1B3 (van de Steeg et al., 2012). Similar to the FCR mice, treatment with CsA significantly suppressed activation and expansion of A6+ and CD44v6+ LPCs (Figures 7D and 7E). Importantly, tumor burden was significantly reduced in $Fah^{-/-}$ mice upon CsA treatment, which displayed lower tumor numbers and smaller average tumor size compared with untreated controls (Figure 7F and data not shown). The decreased tumor burden was also reflected by a significantly reduced overall liver weight (3.1 versus 2.2 g, p ≤ 0.05) (data not shown).

To specifically elaborate the role of CD8+ cells in our model, we exposed 2-month-old $Fah^{-/-}$ mice to two courses of NTBC withdrawal and re-treatment while simultaneously receiving CD8+ cell-depleting ant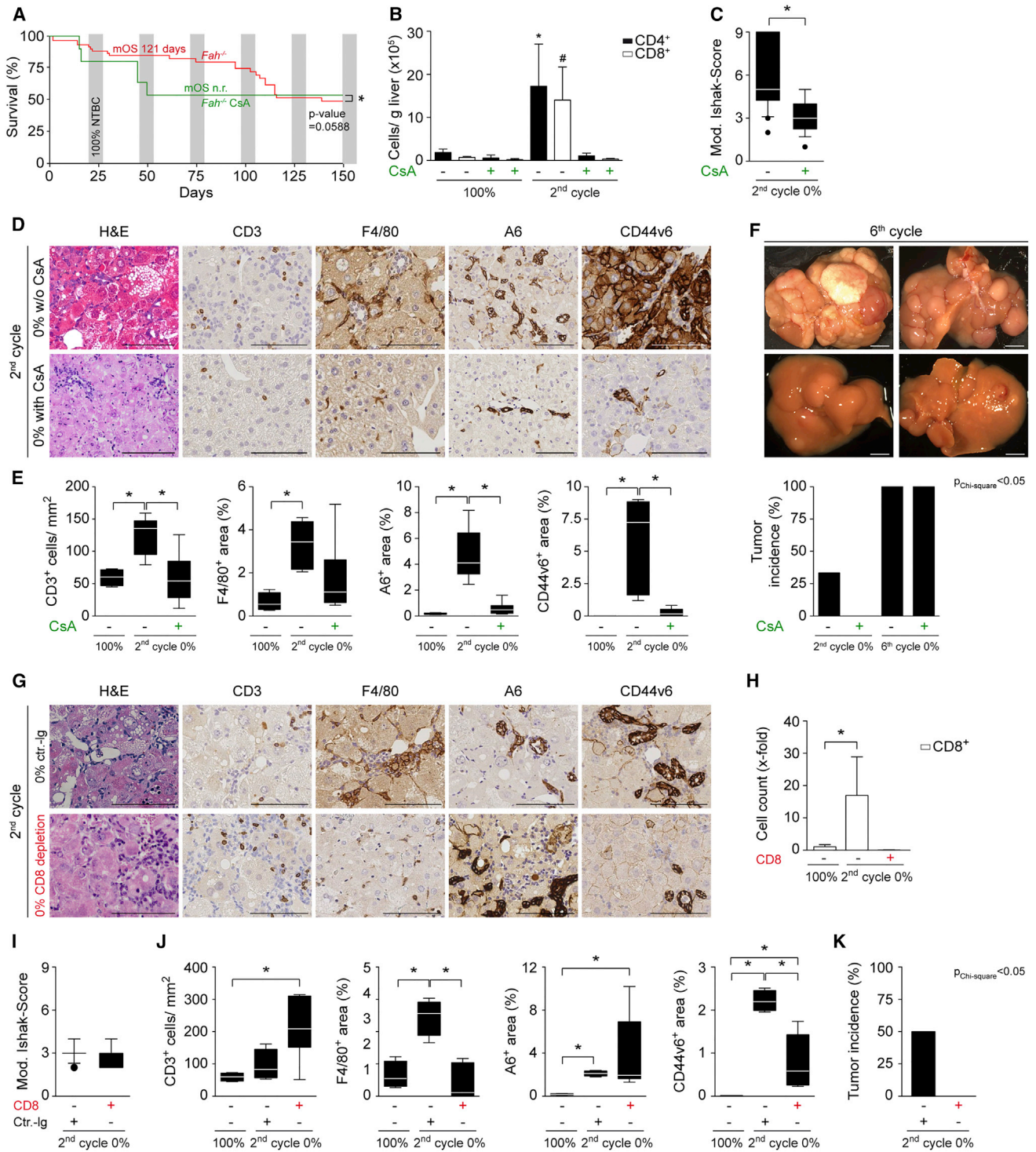ibody. Flow cytometry confirmed a significantly lower number of CD8+ T cells, which was accompanied by a higher number of CD3+ and CD4+ cells (Figures 7G, 7H, 7J, and S4). Liver injury was not significantly reduced by CD8+ T cell depletion (Figure 7I). Interestingly, F4/80+ cells were significantly lower in CD8-depleted $Fah^{-/-}$ mice compared with control mice. In agreement with the observation in Fβ2m mice, A6+ cells were not reduced in CD8+-depleted mice, suggesting that CD8+ cells are not required for the A6+ oval cell response (Figures 7G and 7J). In contrast, CD44v6+ progenitor cells were also significantly reduced in CD8-depleted mice, indicating that CD8+ cells are specifically required for the expansion of putative HCC progenitor cells. None of the CD8+ cell-depleted mice subsequently developed liver tumors (Figure 7K).

Thus, these experiments recapitulate our observations in genetically immunosuppressed mice and further corroborate our hypothesis that activation of CD8+ cells significantly contributes to hepatocarcinogenesis.

CD8+ T Cells Are Required for FAA-Induced Hepatocarcinogenesis

Next, we set out to determine whether tumor development could be delayed in $Fah^{-/-}$ mice by employing a T cell-directed pharmaceutical approach. Cyclosporine A (CsA) is an immunosuppressive drug that blocks activation and expansion of T cells via the inhibition of calcineurin and NFATc signaling. Survival of $Fah^{-/-}$ mice was not significantly compromised upon CsA treatment during NTBC cycling (Figure 7A) (median overall survival not reached, n = 31, HR 0.54, p = 0.0588). As expected, flow cytometric and immunohistochemistry (IHC) analysis confirmed a significantly lower number of CD3+ T cells and a trend toward a lower number of F4/80+ cells in CsA-treated mice compared with control mice (Figures 7B, 7D, and 7E). Impaired T cell activation by CsA treatment reduced biochemical and histological liver damage (Figures 7C and 7D). As previously reported, bilirubin levels increased during CsA treatment (data not shown),

Figure 7. Cyclosporine A Reduces Hepatocarcinogenesis in *Fah*^{−/−} Mice

(A–F) *Fah*^{−/−} mice undergoing daily treatment with CsA were cycled and livers were harvested after the second and sixth cycles. (A) Kaplan-Meier plot showing the survival rates of CsA-treated *Fah*^{−/−} and untreated *Fah*^{−/−} mice. Survival of *Fah*^{−/−} mice was not significantly compromised upon CsA treatment during NTBC cycling. n.r., not reached. (B) CsA treatment efficiently suppressed the increase in CD4⁺ and CD8⁺ T cells in *Fah*^{−/−} mice undergoing NTBC cycling; graphs represent absolute CD4⁺ and CD8⁺ T cell counts per gram of liver. (C) Numerical grading of chronic inflammation was performed according to the modified Ishak Score. (D) Histological liver injury is significantly reduced in CsA-treated *Fah*^{−/−} mice. Representative H&E, CD3 (T cells), F4/80 (myeloid cells), A6, and CD44v6 (LPC response) stainings on liver sections. (E) CD3⁺ cells/mm², and F4/80⁺, A6⁺, and CD44v6⁺ areas were calculated. (F) Tumor burden is reduced in CsA-treated *Fah*^{−/−} mice. Representative macroscopic images of liver explants are shown. Tumor incidence of *Fah*^{−/−} and *Fah*^{−/−} CsA-treated mice were calculated.

(legend continued on next page)

Lymphotoxin-β Receptor Signaling Contributes to Hepatocarcinogenesis in *Fah*^{−/−} Mice

Finally, we aimed to delineate which cytokine mediates the impact of CD8^{+} T cells on hepatocarcinogenesis. To identify pro-tumorigenic signaling cascades in livers of *Fah*^{−/−} mice, we compared gene-expression patterns between tumor-prone *Fah*^{−/−} mice and immunocompromised mice in which tumor development was found to be reduced (CsA-treated *Fah*^{−/−} mice Figure 7F, FCR mice Figures 5B–5E, FCR mice with adoptively transferred T cells Figure 6B, FR mice Figure 6B). Gene profiling identified a cluster of genes including LTβ, Ccl17, Ccl20, and Ccl22, among others (Figure 8A), which segregated with tumor development. Cytokine and chemokine mRNA levels were measured by qRT-PCR to confirm the array data. Specifically, the induction of LTα, LTβ receptor (LTβR), LIGHT, and TRAIL strikingly correlated with tumor development in Fah-deficient mice. Moreover, downstream chemokines of the LTβ pathway such as Ccl20, Ccl17, p100, and TNF-α were significantly induced in tumor-prone *Fah*^{−/−} mice (Figure 8B). LTβ was mainly expressed by CD3^{+} T cells and rarely by hepatocytes and other non-parenchymal immune cells, as shown by LTβ mRNA in situ staining (Figure 8C).

LTβ has previously been shown to induce hepatotoxicity and promote carcinogenesis in the liver (Haybaeck et al., 2009; Wolf et al., 2014). To investigate the role of LTβR in the transition from chronic liver injury to HCC, we blocked LTβ signaling using an LTβ receptor immunoglobulin fusion protein (LTβR-Ig). Two-month-old *Fah*^{−/−} mice were exposed to two courses of NTBC withdrawal and re-treatment while simultaneously receiving LTβR-Ig. LTβR-Ig neither affected survival of mice (Figure 8D) nor altered the relative abundance of T cells within the liver (data not shown). Moreover, we did not observe a significant impact on biochemical and histological liver injury and on the expansion of A6[+] and CD44v6[+] LPCs when compared with *Fah*^{−/−} mice treated with a control antibody (Figures 8E, 8F, and 8G). Notably however, LTβR-Ig significantly suppressed FAA-induced tumor formation compared with control mice (50% versus 8.3%, p ≤ 0.05) and reduced tumor count (2.0 versus 1.0) in LTβR-Ig-treated *Fah*^{−/−} mice (Figure 8H). Reduced tumor burden correlated with decreased expression of LTβ-regulated cytokines such as Ccl17, Ccl20, and TNF-α (data not shown). Together, our results indicate that long-term suppression of LTβR signaling can suppress the transition from dysplastic hepatocytes into HCCs.

DISCUSSION

Hepatocellular carcinoma is one of the most lethal and prevalent cancers worldwide, and frequently arises in the presence of chronic injury and inflammation. It is commonly associated with viral hepatitis, chronic exposure to toxins, or hereditary liver diseases (Kirstein and Vogel, 2014). The immune system serves an important role in guarding organ homeostasis in the face of exposure to toxins and hepatotrophic viruses. Lately, the immune system has increasingly been recognized as a key contributor to tumor initiation and progression, yet the precise molecular mechanisms remain elusive. In this study, we analyze the molecular events occurring during liver cancer initiation using a well-established mouse model of chronic liver injury and hepatocarcinogenesis (Buitrago-Molina et al., 2009, 2013; Grompe et al., 1993; Grompe et al., 1995; Marhenke et al., 2008; Vogel et al., 2004). Our data unveil that apart from their role in maintaining hepatic inflammation, the presence or absence of T cells is decisive for tumor development in chronic liver injury. Mechanistically, we provide evidence that CD8^{+} T cell and LTβ drive the malignant transformation of hepatocytes.

HT1 is caused by genetic inactivation of the last step in tyrosine metabolism leading to the accumulation of the metabolite FAA. FAA is a thiol-reacting and organelle/mitotic spindle-disturbing agent with mutagenic activities. Hence, liver injury in HT1-deficient organisms has been mainly attributed to immediate toxicity of the metabolite (Jorquera and Tanguay, 2001). Our work demonstrates that chronic liver damage and hepatocyte destruction is predominantly mediated by the adaptive immune system. This concept is supported by a presumed role of lymphocytes in mounting an immune response that promotes hepatic damage in diverse liver diseases such as acetaminophen-induced liver failure or chronic hepatitis B and C infection (Adams et al., 2010; Rehermann, 2013).

Although T cells set the stage for chronic liver injury, they actually protect mice from acute-on-chronic liver failure. Consistent with the notion that the adaptive immune system helps to prevent acute liver failure, adoptively transferred T cells reduce the high mortality of immunosuppressed Fah-deficient mice. The exact reason for the high mortality in FCR mice remains elusive. Interestingly, however, acute liver failure in our model closely resembles acute-on-chronic liver failure in humans with chronic liver diseases. Acute-on-chronic liver failure is an increasingly recognized syndrome in patients with chronic liver diseases characterized by acute deterioration of cirrhosis, organ failure, and extremely poor survival (Arroyo et al., 2015). Recent studies indicate that patients who develop acute-on-chronic liver failure have an excessive innate immune response. In 30% of cases the immune response may be triggered by pathogen-associated molecular patterns released by bacteria. Alternatively, the excessive immune response may be a result of pattern recognition receptor activation by non-bacterial molecules released by dying cells. Thus, one may speculate that the adaptive immune system prevents acute liver failure by preventing an excessive response triggered by bacterial and/or non-bacterial molecules.

Liver injury is generally accompanied by compensatory liver regeneration, which can be accomplished through hepatocyte hypertrophy, hepatocyte proliferation, and activation of LPCs.

(G–K) *Fah*^{−/−} mice were exposed to two courses of NTBC withdrawal and simultaneously received CD8^{+} cell-depleting antibody. (G) Representative images and (J) quantification of histology of CD3 (T cells), F4/80 (myeloid cells), A6, and CD44v6 (LPC response) IHC. (H) CD8^{+} cell depletion was confirmed by FACS analysis. (I) The modified Ishak Score did not reveal significant differences between the cohorts. (K) Tumor incidence is significantly reduced in mice with CD8^{+} T cell depletion.

Data represent mean ± SD or median with whiskers from 10th to 90th percentiles. *p ≤ 0.05. Scale bars represent 100 μm, except for macroscopic pictures (5 mm). See also Figure S4.

A

B

C 2nd cycle - 0% NTBC

D

E

F

G

H
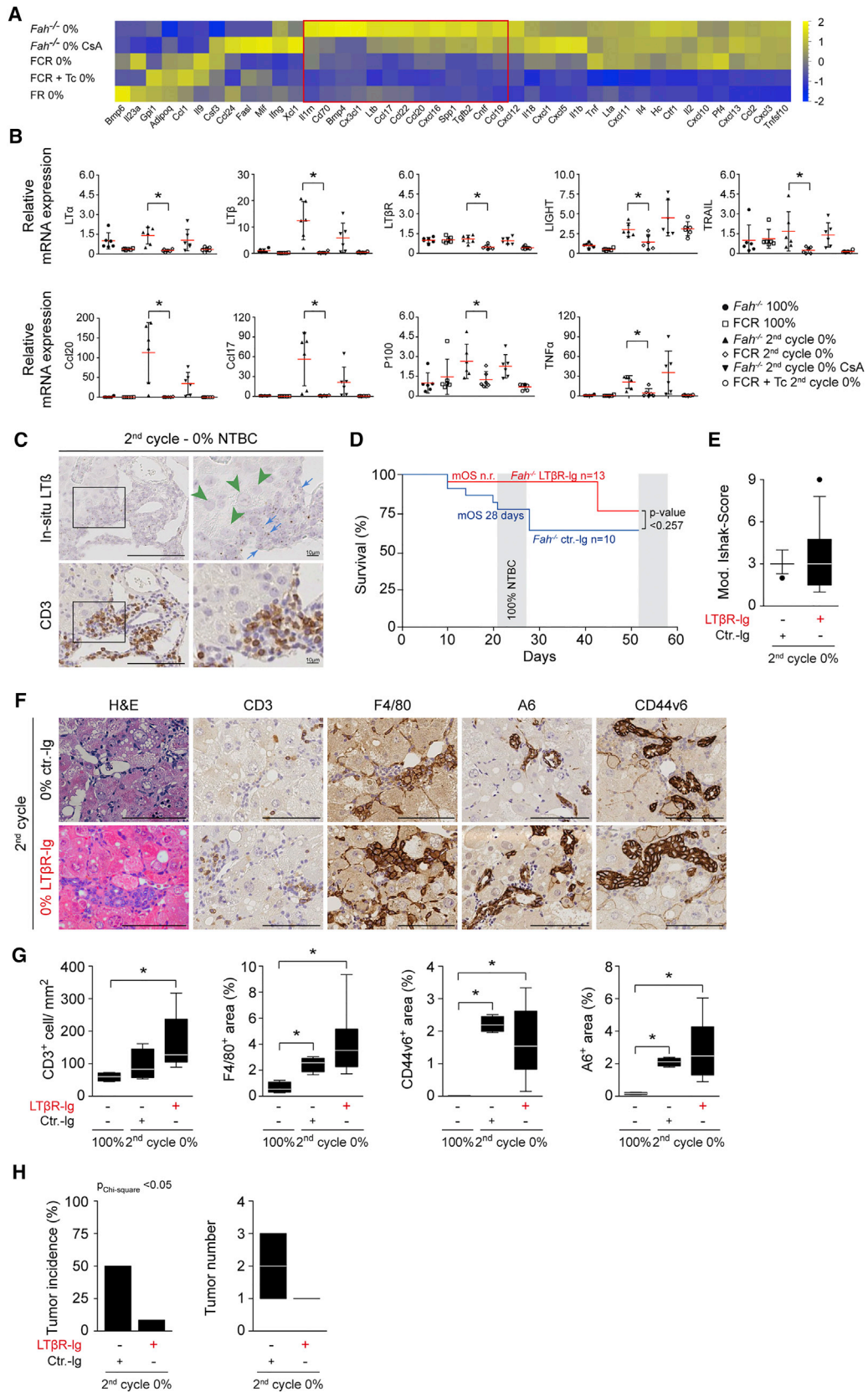
(legend on next page)

Previous studies have suggested that the immune system impairs liver regeneration in healthy mice following PH (Tumanov et al., 2009). Upon provoking chronic liver damage by NTBC withdrawal, immunosuppressed $Fah^{-/-}$ mice exhibit strikingly reduced signs of liver injury and subsequently less liver regeneration compared with fully immunocompetent $Fah^{-/-}$ control mice. To further delineate whether the immune system promotes hepatocyte proliferation in $Fah^{-/-}$ mice, we performed partial hepatectomies and hepatocyte transplantations. Restoration of liver mass was not impaired, nor was mortality increased in healthy, NTBC-supplemented $Fah^{-/-}$ $Rag2^{-/-}$ $Il2r\gamma^{-/-}$ mice following PH. Moreover, in the setting of chronic liver injury, WT hepatocytes re-populated $Fah^{-/-}$ $Rag2^{-/-}$ $Il2r\gamma^{-/-}$ livers to the same extent as $Fah^{-/-}$ livers, suggesting that the adaptive immune system is not required for hepatocyte proliferation. However, in agreement with previous studies, we show that CD4$^+$ T cells are required for activation of LPCs in $Fah^{-/-}$ mice (Strick-Marchand et al., 2008).

FAA-induced liver injury causes rapid onset of HCC in men (Mayorandan et al., 2014). Similarly, Fah-deficient mice develop HCC on low-dose NTBC within 12 months (Marhenke et al., 2008). Human liver diseases are usually characterized by flares of liver injury followed by phases of recovery and regeneration. Therefore, to mimic the human situation we induced repeated flares of liver injury in $Fah^{-/-}$ mice. Alternating phases of injury and regeneration dramatically accelerate tumor development, and lead to multifocal HCCs in all mice within 4 months. aCGH analysis of murine tumors revealed a high number of chromosomal aberrations reflecting increased genomic instability. The shared copy-number alterations across the analyzed tumors suggest a common route of carcinogenesis. Moreover, comparison of genomic alterations in FAA-induced HCCs to human HCCs from the Cancer Genome Atlas database demonstrated gains and losses in chromosomal regions congruent with genomic alterations found in human HCCs.

We postulate that acceleration of tumor onset is most likely related to the strong inflammation-induced proliferative response during the recovery phase. This hypothesis is supported by recent reports showing that the synergistic action of inflammation-induced cell proliferation and DNA-damaging environmental agents cause DNA sequence rearrangements that culminate in cancer formation (Kiraly et al., 2015). Recently, CD44$^+$ HCC progenitor cells were identified in several HCC mouse models (He et al., 2013). In contrast to HCC-derived cancer cells, these progenitor cells solely give rise to tumors in mice with chronic liver injury. In our model, liver sections

from $Fah^{-/-}$ mice showed the progressive appearance of CD44v6$^+$ cells whereas these cells did not increase in immunosuppressed mice, suggesting that FAA-induced liver injury only gives rise to bona fide HCC-initiating cells in immunocompetent mice.

Suppression of the immune system is commonly regarded as a risk factor for the development of de novo malignancies in patients, likely related to an increased susceptibility to infections with oncogenic viruses such as Epstein-Barr or human papilloma viruses (Schrem et al., 2013). Strikingly, tumor development was markedly reduced in genetically immunocompromised $Fah^{-/-}$ mice. This finding was also recapitulated upon pharmacologic inhibition of the adaptive immune system with CsA. Mechanistically, we show that CD8$^+$ T cells and LTβ signaling contributes to tumor development in Fah-deficient mice. Studies on the tumor modulating effects of the immune system in liver carcinogenesis are not yet fully conclusive. In respect of CT4$^+$ T cells and myeloid cells, it has been recently shown that antigen-specific CD4$^+$ T cells orchestrate immune surveillance of pre-malignant hepatocytes in a genetically engineered murine HCC model (Kang et al., 2011). Antibody-mediated depletion of CD4$^+$ T cells also resulted in a strong accumulation of senescent hepatocytes in $Tak1^{-/-}$ mice, which already led to accelerated liver tumor development at 3 months of age in this inflammation-based HCC mouse model. Interestingly, CD4$^+$ T cells act in a T-helper cell manner and require myeloid cells to clear pre-malignant senescent hepatocytes and suppress tumor development. Very recently it has been shown that dysregulation of lipid metabolism causes selective loss of intrahepatic CD4$^+$ T cells, leading to accelerated hepatocarcinogenesis in non-alcoholic fatty liver disease (Ma et al., 2016). In contrast, metabolic activation of intrahepatic NKT and CD8$^+$ T cells by lipids has been shown to induce hepatotoxicity and promote non-alcoholic steatohepatitis-driven hepatocarcinogenesis (Wolf et al., 2014). Together, these data indicate that CD4$^+$ cells and myeloid cells represent an important anti-tumor barrier, whereas our data identify CD8$^+$ T cells as the crucial cellular component of inflammation-associated hepatocarcinogenesis.

LTβ, a central member of the TNF family, is secreted by lymphocytes, whereas LTβR is expressed on hepatocytes, stromal, epithelial, and myeloid cells, implicating that LTβ signaling functions as a critical mediator between lymphocytes and the surrounding parenchymal and immune cells (Browning and French, 2002). Long-term activation of LTβ signaling induces liver inflammation and fosters hepatocarcinogenesis, thereby causally linking hepatic LTβ signaling and tumor development. Notably,

Figure 8. Lymphotoxin-β Mediates the Impact of T Cells on Hepatocarcinogenesis
(A and B) mRNA from total liver was isolated from $Fah^{-/-}$, FCR, T cell transplanted FCR (FCR + Tc), FR and CsA-treated $Fah^{-/-}$ mice after two cycles (0% NTBC). (A) Expression profiling of chemokines and cytokines using the RT^2 PCR Profiler. The red box marks a cluster of differentially regulated genes in tumor-bearing mice, including multiple components of the lymphotoxin signaling pathway. (B) Quantitative analysis of LTβ signaling-related genes, including LTα, LTβ, LTβR, LIGHT, TRAIL, Ccl20, Ccl17, P100, and TNF-α, was performed by qRT-PCR. Relative expression levels were found to be significantly upregulated in $Fah^{-/-}$ compared with FCR mice.
(C–H) $Fah^{-/-}$ mice were treated with LTβR-Ig and respective control antibody (ctr.-Ig) for two NTBC cycles. (C) LTβ is mainly expressed by CD3$^+$ T cells (arrows) and rarely by hepatocytes (arrowheads) and other non-parenchymal immune cells as shown by LTβ mRNA in situ staining. Boxed areas are magnified. (D) Kaplan-Meier plot showing similar overall survival in LTβR-Ig and control-treated mice. (E) Modified Ishak Score indicate similar levels of liver injury in both groups. (F) Histological assessment of LTβR-Ig- and control-treated mice following NTBC withdrawal. No significant differences are observed in the general histological appearance (H&E), T cells (CD3), myeloid cells (F4/80), and LPC response (A6 and CD44v6) (G). (H) Tumor incidence is significantly reduced and tumor number is decreased in livers from LTβR-Ig treated $Fah^{-/-}$ mice.
Data represent mean ± SD or median with whiskers from 10th to 90th percentiles. *p ≤ 0.05. Scale bars represent 100 μm.

expression of LTβ is increased in patients suffering from chronic liver diseases such as chronic hepatitis B and C as well as in human HCC (Haybaeck et al., 2009). Here, treatment with the LTβR-Ig significantly reduced tumor development in $Fah^{-/-}$ mice. Unexpectedly, abrogation of LTβ signaling did not significantly affect the liver progenitor cell compartment in our model, suggesting that LTβ-induced malignant transformation occurs independently of its ability to regulate LPC proliferation.

One limitation of our study is that we have only employed one model. HCC, however, is a very heterogeneous malignancy that develops in a wide variety of chronic liver diseases; different etiological settings cause divergent immune responses, which in turn modulate the progression from chronic injury to HCC in a disease-specific context. Here we use a mouse model of HT1, a human disease, in which the primary injury occurs in hepatocytes and in which immune cells are activated by dysfunctional hepatocytes, similar to the observations made in chronic viral diseases. The model reliably mirrors the inflammatory environment of the human disease, and is therefore suitable to delineate the divergent roles of immune cells in chronic liver injury that sets the stage for tumor development. Currently only few additional models fulfill this prerequisite, each with specific strengths and limitations. Nevertheless, to broadly extrapolate our findings to human HCC in general, similar studies need to recapitulate our findings in other models such as $Mdr2^{-/-}$ mice or mice treated with CCl4 and DEN.

In summary, our results reveal that lymphocytes significantly contribute to liver damage and hepatocarcinogenesis, but also protect mice from acute-on-chronic liver failure and support liver progenitor cell proliferation during chronic liver injury. These findings emphasize the fundamental requirement that the immune system needs to be tightly regulated in a context-specific fashion to balance immune surveillance and cancer risk. Moreover, inhibiting LTβR signaling might be an interesting approach to prevent tumor development in patients with chronic liver diseases accompanied by high levels of LTβ.

EXPERIMENTAL PROCEDURES

Mice

All mouse experiments were performed according to the guidelines and with approval of the Lower Saxony State Office for Consumer Protection and Food Safety (LAVES). B6;129-$Fah^{tm1Mgo}B2m^{tm1Unc}$ (Fβ2m), B6;129-$Fah^{tm1Mgo}Rag2^{tm1Twa}$ (FR), and B6;Cg-$Fah^{tm1Mgo}Rag2^{tm1Fwa}Il2r\gamma^{tm1Wjl}$ (synonym $Fah^{tm1Mgo}Rag2^{tm1Fwa}common\ gamma\ chain^{tm1Wjl}$ = FCR) mice were generated from B6;129-$B2m^{tm1Unc}$, B10;B6-$Rag2^{tm1Fwa}Il2r\gamma^{tm1Wjl}$, and B6;129-$Fah^{tm1Mgo}$ ($Fah^{-/-}$) mice. Animals were kept under standard conditions with a 12-hr day-night cycle and access to food and water ad libitum.

Drinking water was supplemented with (NTBC) at a concentration of 7.5 μg/ml to simulate 100% NTBC treatment. The experimental setup was designed with repeated cycles of NTBC withdrawal and NTBC treatment. In Figure S1 the procedure of the cycling is illustrated. The mortality rate of FCR mice was significantly reduced by treatment with co-trimoxazole during the first two cycles; therefore, these mice were kept under antibiotic treatment for the first two cycles for all subsequent experiments. Thirty mice were similarly treated with co-trimoxazole to exclude a direct effect of co-trimoxazole on the phenotype of $Fah^{-/-}$ mice. There was no effect on survival or tumor incidence compared with untreated cycled $Fah^{-/-}$ mice. To track temporal changes on the quantity and composition of the normal gut microbiota compensation, we performed community fingerprinting approaches based on 16S rRNA gene sequencing from fecal DNA in healthy and cycled $Fah^{-/-}$ mice with and without antibiotic treatment (Figure S5).

Synteny Analysis

To verify the relevance of our mouse model in the human setting, we downloaded the segmented copy-number data of the Liver hepatocellular carcinoma dataset along with the clinical data from the TCGA database. The data were called for copy-number status using the R package CGHcall (van de Wiel et al., 2007) followed by the definition of copy-number regions using the R package CGHregions (van de Wiel and Wieringen, 2007). Synteny analysis was conducted as described in Wolf et al. (2014) for the copy-number regions obtained for the mouse model and for the following human hepatocellular data subsets: alcohol consumption derived, virus-derived, and MYC-alteration derived. To assess the goodness of comparability, we calculated the percentage of gains and losses in the mouse model that were also present in the human subsets of data. Furthermore, the overlap of copy-number changes between mouse model and human data was examined for statistical significance using Fisher's exact test based on the null hypothesis "the overlap between copy-number alterations in mouse model and human data occurred by chance."

Statistical Analysis

Data were analyzed by Student's t test, chi-square, and two-sided nonparametric Mann-Whitney test to determine significance. p Values were considered statistically significant at a level of $p \leq 0.05$. Kaplan-Meier survival analysis was performed on experimental mice; median overall survival and HR were calculated.

ACCESSION NUMBERS

Raw microarray data produced in this paper can be found in the Gene Exression Omnibus under the accession number GEO: GSE80459.

SUPPLEMENTAL INFORMATION

Supplemental Information includes Supplemental Experimental Procedures, five figures, and two tables and can be found with this article online at http://dx.doi.org/10.1016/j.ccell.2016.06.009.

AUTHOR CONTRIBUTIONS

Conceptualization, A.V.; Methodology, A.V., L.E.B.-M., S.M., A.W., M.H., F.L., C.K., and M.P.M.; Investigation, J.E., L.E.B.-M., S.M., F.R., J.S., A.S., A.M., A.C.M., M.E.H., R.G., T.C., D.H., K.U., M.F., and T.L.; Formal Analysis, T.C., D.H., F.R., and R.G.; Validation, L.E.B-M. and S.M.; Visualization, J.E., L.E.B.-M., and S.M.; Writing – Original Draft, A.V.; Writing – Review & Editing, A.V., A.S., L.E.B.-M., S.M., and M.H.; Funding Acquisition, A.V. and M.H.; Supervision, A.V., M.H., A.W., and M.P.M.; Resources, A.V., A.W., M.H., and M.P.M.

ACKNOWLEDGMENTS

REFERENCES

Adams, D.H., Ju, C., Ramaiah, S.K., Uetrecht, J., and Jaeschke, H. (2010). Mechanisms of immune-mediated liver injury. Toxicol. Sci. *115*, 307–321.

Arroyo, V., Moreau, R., Jalan, R., and Gines, P.; EASL-CLIF Consortium CANONIC Study (2015). Acute-on-chronic liver failure: a new syndrome that will re-classify cirrhosis. J. Hepatol. *62*, S131–S143.

Browning, J.L., and French, L.E. (2002). Visualization of lymphotoxin-beta and lymphotoxin-beta receptor expression in mouse embryos. J. Immunol. *168*, 5079–5087.

Buitrago-Molina, L.E., Pothiraju, D., Lamle, J., Marhenke, S., Kossatz, U., Breuhahn, K., Manns, M.P., Malek, N., and Vogel, A. (2009). Rapamycin delays tumor development in murine livers by inhibiting proliferation of hepatocytes with DNA damage. Hepatology *50*, 500–509.

Buitrago-Molina, L.E., Marhenke, S., Longerich, T., Sharma, A.D., Boukouris, A.E., Geffers, R., Guigas, B., Manns, M.P., and Vogel, A. (2013). The degree of liver injury determines the role of p21 in liver regeneration and hepatocarcinogenesis in mice. Hepatology *58*, 1143–1152.

Dorrell, C., Erker, L., Schug, J., Kopp, J.L., Canaday, P.S., Fox, A.J., Smirnova, O., Duncan, A.W., Finegold, M.J., Sander, M., et al. (2011). Prospective isolation of a bipotential clonogenic liver progenitor cell in adult mice. Genes Dev. *25*, 1193–1203.

El-Serag, H.B., Marrero, J.A., Rudolph, L., and Reddy, K.R. (2008). Diagnosis and treatment of hepatocellular carcinoma. Gastroenterology *134*, 1752–1763.

Grompe, M., Al-Dhalimy, M., Finegold, M., Ou, C.N., Burlingame, T., Kennaway, N.G., and Soriano, P. (1993). Loss of fumarylacetoacetate hydrolase is responsible for the neonatal hepatic dysfunction phenotype of lethal albino mice. Genes Dev. *7*, 2298–2307.

Grompe, M., Lindstedt, S., al-Dhalimy, M., Kennaway, N.G., Papaconstantinou, J., Torres-Ramos, C.A., Ou, C.N., and Finegold, M. (1995). Pharmacological correction of neonatal lethal hepatic dysfunction in a murine model of hereditary tyrosinaemia type I. Nat. Genet. *10*, 453–460.

Haybaeck, J., Zeller, N., Wolf, M.J., Weber, A., Wagner, U., Kurrer, M.O., Bremer, J., Iezzi, G., Graf, R., Clavien, P.A., et al. (2009). A lymphotoxin-driven pathway to hepatocellular carcinoma. Cancer Cell *16*, 295–308.

He, G., Dhar, D., Nakagawa, H., Font-Burgada, J., Ogata, H., Jiang, Y., Shalapour, S., Seki, E., Yost, S.E., Jepsen, K., et al. (2013). Identification of liver cancer progenitors whose malignant progression depends on autocrine IL-6 signaling. Cell *155*, 384–396.

Jorquera, R., and Tanguay, R.M. (2001). Fumarylacetoacetate, the metabolite accumulating in hereditary tyrosinemia, activates the ERK pathway and induces mitotic abnormalities and genomic instability. Hum. Mol. Genet. *10*, 1741–1752.

Kang, T.W., Yevsa, T., Woller, N., Hoenicke, L., Wuestefeld, T., Dauch, D., Hohmeyer, A., Gereke, M., Rudalska, R., Potapova, A., et al. (2011). Senescence surveillance of pre-malignant hepatocytes limits liver cancer development. Nature *479*, 547–551.

Kiraly, O., Gong, G., Olipitz, W., Muthupalani, S., and Engelward, B.P. (2015). Inflammation-induced cell proliferation potentiates DNA damage-induced mutations in vivo. PLoS Genet. *11*, e1004901.

Kirstein, M.M., and Vogel, A. (2014). The pathogenesis of hepatocellular carcinoma. Dig. Dis. *32*, 545–553.

Ma, C., Kesarwala, H., Eggert, T., Medina-Echeverz, J., Kleiner, D.E., Jin, P., Stroncek, D.F., Terabe, M., Kapoor, V., ElGindi, M., et al. (2016). NAFLD causes selective CD4+ T lymphocyte loss and promotes hepatocarcinogenesis. Nature *351*, 253–257.

Marhenke, S., Lamle, J., Buitrago-Molina, L.E., Canon, J.M., Geffers, R., Finegold, M., Sporn, M., Yamamoto, M., Manns, M.P., Grompe, M., and Vogel, A. (2008). Activation of nuclear factor E2-related factor 2 in hereditary tyrosinemia type 1 and its role in survival and tumor development. Hepatology *48*, 487–496.

Mayorandan, S., Meyer, U., Gokcay, G., Segarra, N., de Baulny, O., van Spronsen, F., Zeman, J., de Laet, C., Spiekerkötter, U., Thimm, E., et al.

(2014). Cross-sectional study of 168 patients with hepatorenal tyrosinaemia and implications for clinical practice. Orphanet J. Rare Dis. *9*, 107.

Pikarsky, E., Porat, R.M., Stein, I., Abramovitch, R., Amit, S., Kasem, S., Gutkovich-Pyest, E., Urieli-Shoval, S., Galun, E., and Ben-Neriah, Y. (2004). NF-kappaB functions as a tumour promoter in inflammation-associated cancer. Nature *431*, 461–466.

Rehermann, B. (2013). Pathogenesis of chronic viral hepatitis: differential roles of T cells and NK cells. Nat. Med. *19*, 859–868.

Schneider, C., Teufel, A., Yevsa, T., Staib, F., Hohmeyer, A., Walenda, G., Zimmermann, H.W., Vucur, M., Huss, S., Gassler, N., et al. (2012). Adaptive immunity suppresses formation and progression of diethylnitrosamine-induced liver cancer. Gut *61*, 1733–1743.

Schrem, H., Kurok, M., Kaltenborn, A., Vogel, A., Walter, U., Zachau, L., Manns, M.P., Klempnauer, J., and Kleine, M. (2013). Incidence and long-term risk of de novo malignancies after liver transplantation with implications for prevention and detection. Liver Transpl. *19*, 1252–1261.

Strick-Marchand, H., Morosan, S., Charneau, P., Kremsdorf, D., and Weiss, M.C. (2004). Bipotential mouse embryonic liver stem cell lines contribute to liver regeneration and differentiate as bile ducts and hepatocytes. Proc. Natl. Acad. Sci. USA *101*, 8360–8365.

Strick-Marchand, H., Masse, G.X., Weiss, M.C., and Di Santo, J.P. (2008). Lymphocytes support oval cell-dependent liver regeneration. J. Immunol. *181*, 2764–2771.

Tarlow, B.D., Pelz, C., Naugler, W.E., Wakefield, L., Wilson, E.M., Finegold, M.J., and Grompe, M. (2014). Bipotential adult liver progenitors are derived from chronically injured mature hepatocytes. Cell Stem Cell *15*, 605–618.

Tumanov, A.V., Koroleva, E.P., Christiansen, P.A., Khan, M.A., Ruddy, M.J., Burnette, B., Papa, S., Franzoso, G., Nedospasov, S.A., Fu, Y.X., and Anders, R.A. (2009). T cell-derived lymphotoxin regulates liver regeneration. Gastroenterology *136*, 694–704.e4.

van de Steeg, E., Stranecky, V., Hartmannova, H., Noskova, L., Hrebicek, M., Wagenaar, E., van Esch, A., de Waart, D.R., Oude Elferink, R.P., Kenworthy, K.E., et al. (2012). Complete OATP1B1 and OATP1B3 deficiency causes human Rotor syndrome by interrupting conjugated bilirubin reuptake into the liver. J. Clin. Invest. *122*, 519–528.

van de Wiel, M.A., and Wieringen, W.N. (2007). CGHregions: dimension reduction for array CGH data with minimal information loss. Cancer Inform. *3*, 55–63.

van de Wiel, M.A., Kim, K.I., Vosse, S.J., van Wieringen, W.N., Wilting, S.M., and Ylstra, B. (2007). CGHcall: calling aberrations for array CGH tumor profiles. Bioinformatics *23*, 892–894.

Vogel, A., van Den Berg, I.E., Al-Dhalimy, M., Groopman, J., Ou, C.N., Ryabinina, O., Iordanov, M.S., Finegold, M., and Grompe, M. (2004). Chronic liver disease in murine hereditary tyrosinemia type 1 induces resistance to cell death. Hepatology *39*, 433–443.

Willenbring, H., Bailey, A.S., Foster, M., Akkari, Y., Dorrell, C., Olson, S., Finegold, M., Fleming, W.H., and Grompe, M. (2004). Myelomonocytic cells are sufficient for therapeutic cell fusion in liver. Nat. Med. *10*, 744–748.

Willenbring, H., Sharma, A.D., Vogel, A., Lee, A.Y., Rothfuss, A., Wang, Z., Finegold, M., and Grompe, M. (2008). Loss of p21 permits carcinogenesis from chronically damaged liver and kidney epithelial cells despite unchecked apoptosis. Cancer Cell *14*, 59–67.

Wolf, M.J., Adili, A., Piotrowitz, K., Abdullah, Z., Boege, Y., Stemmer, K., Ringelhan, M., Simonavicius, N., Egger, M., Wohlleber, D., et al. (2014). Metabolic activation of intrahepatic CD8(+) T cells and NKT cells causes nonalcoholic steatohepatitis and liver cancer via cross-talk with hepatocytes. Cancer Cell *26*, 549–564.